

ICONN 2015 [4<sup>th</sup> - 6<sup>th</sup> Feb 2015]

International Conference on Nanoscience and Nanotechnology-2015  
SRM University, Chennai, India

## Synthesis of Zinc Ferrite ( $ZnFe_2O_4$ ) Nanoparticles with Different Capping Agents

M. Maria Angelin Sinthiya<sup>1</sup>, K. Ramamurthi<sup>1\*</sup>, S. Mathuri<sup>1</sup>, T. Manimozhi<sup>1</sup>,  
N. Kumaresan<sup>1</sup>, Mudaliar Mahesh Margoni<sup>1</sup>, PC. Karthika<sup>1</sup>

<sup>1</sup>Crystal Growth and Thin Film Laboratory, Department of Physics and Nanotechnology, Faculty of Engineering and Technology, SRM University, Kattankulathur- 603203, Kancheepuram Dt., Tamilnadu, India

**Abstract :** Zinc Ferrite ( $ZnFe_2O_4$ ) nanoparticles were prepared by the hydrothermal method using Poly Ethylene Glycol (PEG) and Cetyl Trimethylammonium Bromide (CTAB) capping agents. X-ray diffraction pattern shows that synthesized nanoparticles exhibit mixed phase of ZnO and  $ZnFe_2O_4$ . Field Emission Scanning Electron Microscopic (FESEM) images revealed that the synthesized nanoparticles of the mixed phase possess agglomerate bunch of square shaped structures. The optical bandgap energy of PEG:  $ZnFe_2O_4$  is relatively less than that of CTAB:  $ZnFe_2O_4$  nanoparticles. Vibrating Sample Magnetometer (VSM) studies confirmed the superparamagnetic behavior of the synthesized samples at room temperature.

**Keywords:** Zinc Ferrite; Capping agents; Hydrothermal Method; Super paramagnetic

### Introduction

Synthesis of the nano materials and various nano structures is attracted the attention due to their surface effect and quantum confinement effect. These factors are modifying the physical and chemical properties of nanomaterials as compared to that of the bulk materials<sup>1</sup>. Currently, magnetic nanoparticles are attracting the attention of researchers because of their extensive applications. The metal spinel ferrites belong to the face centered (fcc) close packing structure of  $AB_2O_4$  type in which A occupies tetrahedralsite, B occupies octahedral cationsite and O occupies the oxygen anionsite<sup>2</sup>. Among the spinel ferrite compounds Zinc Ferrite ( $ZnFe_2O_4$ ) exhibits superparamagnetic behavior and it has potential application in many fields, such as photocatalysis<sup>3</sup>, magnetic resonance imaging (MRI)<sup>4</sup>, Li-ion batteries<sup>5</sup> and gas sensors<sup>6</sup>. Various synthesis methods are proposed to prepare  $ZnFe_2O_4$  nanoparticles such as co-precipitation<sup>2</sup>, combustion<sup>3</sup>, thermal decomposition<sup>7</sup>, solvothermal<sup>8</sup>, hydrothermal<sup>9</sup>, ball milling<sup>10</sup>, and ceramic route<sup>11</sup> techniques. Among the synthesis methods the hydrothermal method has been widely used, because of its simplicity, low cost, nontoxic route and yields crystalline nanomaterials in a short time. In this work superparamagnetic  $ZnFe_2O_4$  nanoparticles were synthesized by hydrothermal method using the capping agents (1) Poly Ethylene Glycol (PEG) and (2) Cetyl Trimethylammonium Bromide (CTAB)). The effect of the PEG and CTAB capping agents on the structural, optical, morphological and magnetic properties of the prepared  $ZnFe_2O_4$  nanoparticle is presented.

## Experimental

ZnFe<sub>2</sub>O<sub>4</sub> nanoparticles were prepared by hydrothermal method using PEG and CTAB capping agents. 4.87 g of ferric nitrate (Fe(NO<sub>3</sub>)<sub>3</sub>), 3.75 g of zinc nitrate (Zn(NO<sub>3</sub>)<sub>2</sub>) and 3.28 g of sodium hydroxide (NaOH) were mixed together and dissolved in 40 ml of distilled water. Then 2 ml of PEG was added drop wise in the solution under constant stirring at room temperature and the pH level was maintained at 11. The mixture was continuously stirred for half an hour and transferred to 50 ml of teflon lined autoclave. The autoclave was sealed and maintained at 165°C for 16 hours in the furnace and then allowed to reach the room temperature. Finally the brown precipitated solution was washed several times with distilled water and absolute ethanol. Then the brown precipitates were collected and dried at 60°C for 6 hours in hot air oven and characterized. The same procedure was followed to prepare ZnFe<sub>2</sub>O<sub>4</sub> nanoparticles using the CTAB capping agent. 4.79 g of ferric nitrate, 3.78 g of zinc nitrate, 3.30 g of sodium hydroxide and 2 g of CTAB were used. ZnFe<sub>2</sub>O<sub>4</sub> nanoparticles prepared with the capping agents PEG and CTAB are named as (a) PEG: ZnFe<sub>2</sub>O<sub>4</sub> and (b) CTAB: ZnFe<sub>2</sub>O<sub>4</sub> and used in the discussion.

## Results and Discussion

### Structural analysis

The crystallographic structure of the synthesized ZnFe<sub>2</sub>O<sub>4</sub> nanoparticles was identified by powder X-Ray Diffraction (XRD) measurement. The powder XRD patterns of PEG: ZnFe<sub>2</sub>O<sub>4</sub> and CTAB: ZnFe<sub>2</sub>O<sub>4</sub> are presented in Fig.1. The XRD peaks of the prepared samples were indexed by comparing with the JCPDS card No: 22-1012 which confirms the formation of ZnFe<sub>2</sub>O<sub>4</sub>. XRD pattern shows that synthesized nanoparticles exhibit mixed phase of ZnO and ZnFe<sub>2</sub>O<sub>4</sub> where the ZnFe<sub>2</sub>O<sub>4</sub> belongs to face centered regular spinel cubic structure. The XRD peak indexed at 2θ=35.19° in Fig.1a and at 2θ= 35.14° in Fig.1b corresponds to (3 1 1) plane of ZnFe<sub>2</sub>O<sub>4</sub>. The diffraction peak of ZnO was indexed by comparing with the JCPDS card no: 89-1397. The predominant (1 0 1) XRD peak at 2θ=36.3° corresponds to the ZnO belonging to the primitive hexagonal structure.

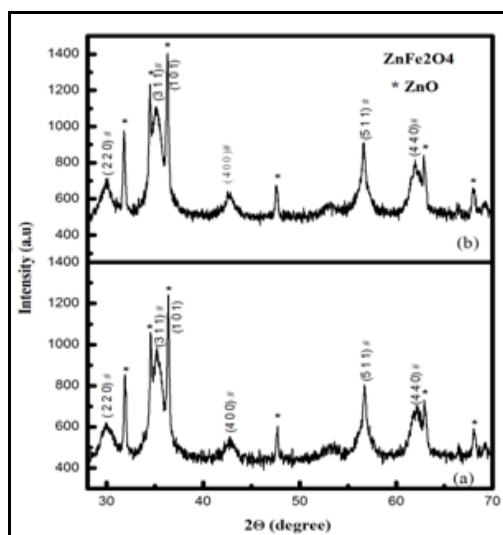


Fig.1 XRD patterns of (a) PEG: ZnFe<sub>2</sub>O<sub>4</sub> and (b) CTAB: ZnFe<sub>2</sub>O<sub>4</sub> of nanoparticles

(# indicates the ZnFe<sub>2</sub>O<sub>4</sub> and \* indicates the ZnO)

The crystallite size (D) was calculated using Scherrer's equation,  $D = k\lambda / (\beta \cos\theta)$ , where k is a constant 0.89,  $\theta$  is the Bragg's diffraction angle,  $\beta$  is full width half maximum (in radians), and  $\lambda$  is the wavelength of X-rays used (1.5406 Å). The broadening of the X-ray diffraction pattern gives clear evidence for the nanocrystalline nature of the synthesized samples. The crystallite size was calculated from the peak (311) of the ZnFe<sub>2</sub>O<sub>4</sub> nanoparticles. The lattice parameter calculated in this work from PEG: ZnFe<sub>2</sub>O<sub>4</sub> nanoparticles is  $a = 8.436$  Å and from CTAB: ZnFe<sub>2</sub>O<sub>4</sub> nanoparticles is  $a = 8.461$  Å. The value of crystallite size calculated for PEG: ZnFe<sub>2</sub>O<sub>4</sub> and CTAB: ZnFe<sub>2</sub>O<sub>4</sub> is 6.6 nm and 7.1 nm respectively.

### Optical analysis

The optical property of the synthesized  $\text{ZnFe}_2\text{O}_4$  nanoparticles was investigated by UV-Visible absorption spectrum. Fig.2 shows that the UV-Visible absorption spectra of the as-synthesized  $\text{ZnFe}_2\text{O}_4$  nanoparticles recorded in the range of wavelength 200-800 nm. The optical spectrum shows the absorption peak of PEG:  $\text{ZnFe}_2\text{O}_4$  at  $\sim 333$  nm and that of CTAB:  $\text{ZnFe}_2\text{O}_4$  at  $\sim 369$  nm. When comparing the absorption peak of PEG:  $\text{ZnFe}_2\text{O}_4$ , the CTAB:  $\text{ZnFe}_2\text{O}_4$  absorption peak is shifted towards the higher wavelength. The calculated bandgap ( $E_g$ ) of PEG:  $\text{ZnFe}_2\text{O}_4$  and CTAB:  $\text{ZnFe}_2\text{O}_4$  nanoparticles is  $\sim 3.05$  eV and  $\sim 3.51$  eV respectively.

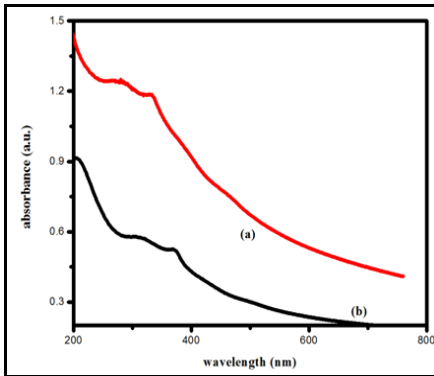


**Fig.2 Optical Absorption Spectrum Of (a) PEG:  $\text{ZnFe}_2\text{O}_4$  and (b) CTAB:  $\text{ZnFe}_2\text{O}_4$  nanoparticles**

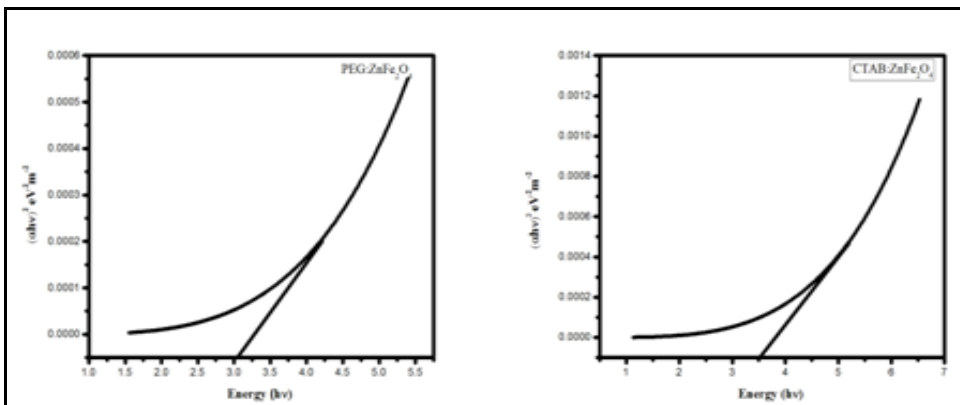


**Fig .3 Plot of  $h\nu$  vs  $(\alpha h\nu)^2$  for (a) PEG:  $\text{ZnFe}_2\text{O}_4$  and (b) CTAB:  $\text{ZnFe}_2\text{O}_4$  nanoparticles**

### Morphology and Elemental Analysis

The morphology of the prepared  $\text{ZnFe}_2\text{O}_4$  nanoparticles was investigated by FE-SEM. The FE-SEM image of (a) PEG:  $\text{ZnFe}_2\text{O}_4$  and (b) CTAB:  $\text{ZnFe}_2\text{O}_4$  nanoparticles is shown in Figs.4a,b respectively. The FE-SEM images exhibit agglomerated bunch of square shaped nanoparticles. The small size of nanoparticles leads to high agglomeration because of its high surface energy<sup>9</sup>. The FE-SEM image shows that the agglomeration of PEG: $\text{ZnFe}_2\text{O}_4$  nanoparticle is relatively higher when compared to that of the CTAB:  $\text{ZnFe}_2\text{O}_4$  nanoparticles because of the effect of capping agent on modifying crystal sizes. It is difficult to determine the exact size of the particle using FE-SEM because most of the particles are agglomerated<sup>12</sup>.

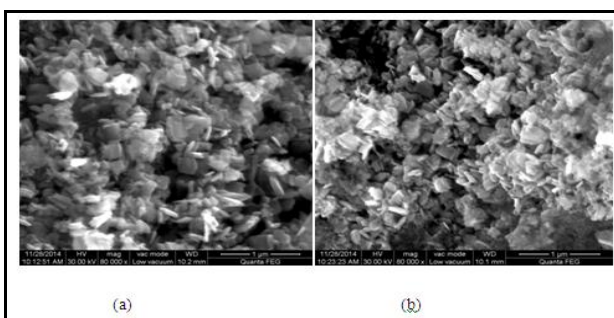


**Fig.4 FE-SEM images of (a) PEG:  $\text{ZnFe}_2\text{O}_4$  and (b) CTAB:  $\text{ZnFe}_2\text{O}_4$  nanoparticles**

The elemental composition of prepared  $\text{ZnFe}_2\text{O}_4$  nano materials investigated by EDAX is shown in Fig.5a for PEG:  $\text{ZnFe}_2\text{O}_4$  and in Fig.5b for CTAB:  $\text{ZnFe}_2\text{O}_4$ . The EDAX spectrum confirms the presence of Zn, Fe and O in the synthesized nanoparticles. The atomic and weight percentages of PEG:  $\text{ZnFe}_2\text{O}_4$  and CTAB:  $\text{ZnFe}_2\text{O}_4$  are presented in the Table.1.

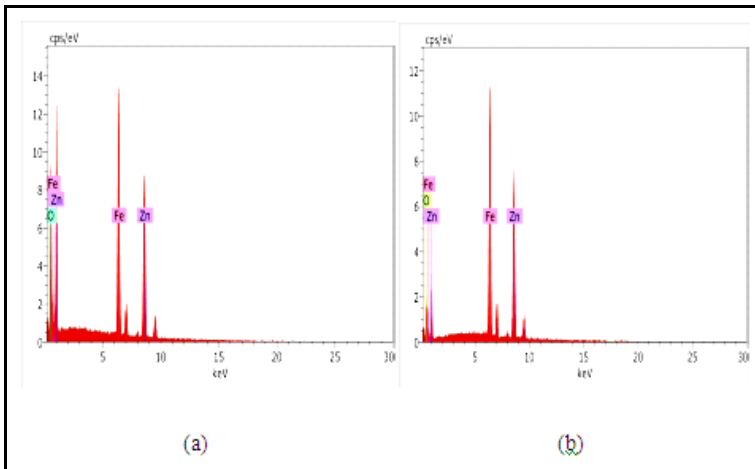


Fig.5 EDAX spectra of (a) PEG:  $\text{ZnFe}_2\text{O}_4$  and (b) CTAB:  $\text{ZnFe}_2\text{O}_4$  nanoparticles

Table.1 Elemental composition from EDAX spectral analysis

Elements	Series	PEG: $\text{ZnFe}_2\text{O}_4$		CTAB: $\text{ZnFe}_2\text{O}_4$	
		Weight percentage	Atomic percentage	Weight percentage	Atomic percentage
Zn	K-series	30.92	13.65	43.62	26.56
Fe	K-series	29.75	15.38	37.68	26.87
O	K-series	39.33	70.97	18.71	46.57
Total		100	100	100	100

### Magnetic properties of $\text{ZnFe}_2\text{O}_4$

Magnetic hysteresis loop (M.H loop) was recorded employing the vibrating sample magnetometer (VSM). Fig.6 shows the hysteresis loops of the  $\text{ZnFe}_2\text{O}_4$  nanoparticles recorded at room temperature. The coercivities of  $\text{ZnFe}_2\text{O}_4$  nanoparticles for the two samples are almost negligible and the remanent magnetization ( $M_r$ ) of PEG:  $\text{ZnFe}_2\text{O}_4$  and CTAB:  $\text{ZnFe}_2\text{O}_4$  is 0.0003emu/g and 0.0007emu/g respectively. Thus the results clearly indicate the superparamagnetic behavior of the prepared samples due to decrease in the particle size below a critical value (lower than 100 nm)<sup>13</sup>. The saturation magnetization ( $M_s$ ) value of PEG:  $\text{ZnFe}_2\text{O}_4$  and CTAB:  $\text{ZnFe}_2\text{O}_4$  is 1.72 emu/g and 1.92 emu/g respectively. The higher crystal size gives higher magnetization<sup>14</sup>. In this work the XRD results indicate that the crystal size of PEG:  $\text{ZnFe}_2\text{O}_4$  is relatively smaller than that of CTAB:  $\text{ZnFe}_2\text{O}_4$  hence the magnetization value of PEG:  $\text{ZnFe}_2\text{O}_4$  is smaller than that of the CTAB:  $\text{ZnFe}_2\text{O}_4$  (Fig.6). The size of the crystalline nature influences the magnetic properties of the nanoparticles.

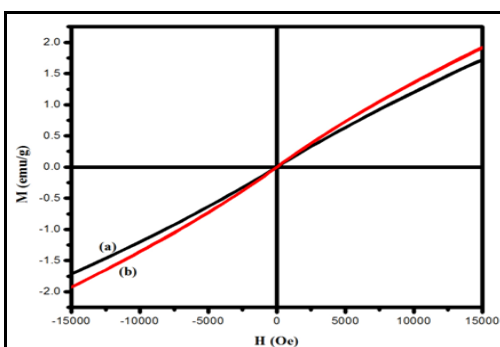


Fig. 6 Hysteresis curves for (a) PEG:  $\text{ZnFe}_2\text{O}_4$  and (b) CTAB:  $\text{ZnFe}_2\text{O}_4$  nanoparticles at room temperature.

## Conclusion

Superparamagnetic ZnFe<sub>2</sub>O<sub>4</sub> nanoparticles were successfully prepared by hydrothermal method using PEG and CTAB capping agents. The powder XRD analysis revealed presence of the mixed phases of ZnFe<sub>2</sub>O<sub>4</sub> and ZnO in the synthesized nanomaterials. The ZnFe<sub>2</sub>O<sub>4</sub> belongs to face centered regular spinel cubic structure, and ZnO belongs to primitive hexagonal structure. XRD studies show that the PEG reduces the crystallite size to 6.6 nm which is relatively smaller than the size of 7.1 nm yielded by CTAB. FE-SEM images exhibit agglomerated bunch of square shaped ZnFe<sub>2</sub>O<sub>4</sub> nanoparticles and the EDAX spectrum confirms the presence of Zn, Fe and O in the synthesized nanoparticles. VSM measurements confirmed the superparamagnetic behavior of the synthesized samples at room temperature and the effect of crystallite size on the magnetic properties. The optical bandgap energy of PEG: ZnFe<sub>2</sub>O<sub>4</sub> is relatively less than that of CTAB: ZnFe<sub>2</sub>O<sub>4</sub> nanoparticles. Thus the present work concludes that the PEG and CTAB capping agents influence the structural, magnetic and optical properties of synthesized ZnFe<sub>2</sub>O<sub>4</sub> nanoparticles, and the PEG capping agent has more influence on the particle size and hence the properties of the ZnFe<sub>2</sub>O<sub>4</sub> nanoparticles.

## Acknowledgements

One of the authors M.Maria Angelin Sinthiya sincerely thanks SRM University, Chennai for the award of SRM fellowship to carry out the research work. The authors gratefully acknowledge Prof. D. John Thiruvadigal, Head, Department of Physics & Nanotechnology, SRM University, Chennai for extending (DST-FIST (SR/FST/PSI-155/2010)) facilities to characterize the prepared nanoparticles and also thanks Nanotechnology Research Centre (NRC), and Dr.Nepolean, SRM Research Institute and Indian Institute of Technology (Chennai) for XRD, FE-SEM, EDAX, UV-Visible and VSM measurements.

## References

1. Mahmoud Goodarz Naseri, Elias B, Saion, Ahmad Kamali, An overview on Nanocrystalline ZnFe<sub>2</sub>O<sub>4</sub>, MnFe<sub>2</sub>O<sub>4</sub> and CoFe<sub>2</sub>O<sub>4</sub> synthesized by a Thermal Treatment Method, ISRN Nanotechnology, 2012, 2012, 1-11.
2. Ebrahim M, Raeisi Shahraki R, Seyyed Ebrahim S.A., Masoudpanah S.M. Magnetic Properties of Zinc Ferrite Nanoparticles Synthesized by Coprecipitation Method. , J Supercond Nov Magn, 2014, 27, 1587–1592.
3. Song Sun, Xiaoyan Yang, Yi Zhang, Fan Zhang, Jianjun Ding, Jun Bao , Chen Gao, Enhanced photocatalytic activity of sponge-like ZnFe<sub>2</sub>O<sub>4</sub> synthesized by solution combustion method, Progress in Natural Science: Materials International, 2012, 22, 639–643.
4. Wan J, Jiang X, Li H, Chen K, Facile Synthesis of Zinc Ferrite nanoparticles as non-lanthanide T1 MRI contrast agents, J. Mater. Chem. 2012, 22, 13500-13505.
5. Lin Lian, Linrui Hou, Lu Zhou, Lishi Wangb and Changzhou Yuan, Rapid low-temperature synthesis of mesoporous nanophase ZnFe<sub>2</sub>O<sub>4</sub> with enhanced lithium storage properties for Li-ion batteries, RSC Adv., 2014, 4, 49212–49218.
6. Shurong Wang, Xueling Gao, Jiedi Yang, Zhenyu Zhu, Hongxin Zhang, and Yanshuang Wang, Synthesis and gas sensor application of ZnFe<sub>2</sub>O<sub>4</sub> – ZnO composite hollow microspheres, RSC Advances, 2014, 1-10.
7. Kalpanadevi Kalimuthu, Sinduja C. Rangasamy, Manimekalai Rakkiyasamy, Characterization of ZnFe<sub>2</sub>O<sub>4</sub> nanoparticles obtained by the Thermal Decomposition of ZnFe<sub>2</sub>(cin)<sub>3</sub>(N<sub>2</sub>H<sub>4</sub>)<sub>3</sub>, Acta Chim. Slov. 2013, 60, 896–900.
8. Blanco-Gutierrez V, Torralvo MJ, Saez-Puche R, Bonville P, Magnetic properties of solvothermally synthesized ZnFe<sub>2</sub>O<sub>4</sub> nanoparticles, Journal of physics, 2010, 200, 1742-6596.
9. Rameshbabu R, Ramesh R, Kanagesan S, Karthigeyan A, Ponnusamy S, Synthesis and study of structural, morphological and magnetic properties of ZnFe<sub>2</sub>O<sub>4</sub> nanoparticles, J.supercond Nov Magn, 2014, 27, 1499-1502.
10. Mozaffari M, Masoudi H, Zinc Ferrite nanoparticles: New preparation method and magnetic properties, J Supercond Nov Magn, 2014, 27, 2563–2567.
11. Mohammad Niyafar, Effect of preparation on structure and magnetic properties of ZnFe<sub>2</sub>O<sub>4</sub>, Journal of Magnetism, 2014, 19(2), 101-105.
12. Prithviraj Swamy P.M, Basavaraja S, Arunkumar Lagashetty, Srinivas Rao N.V, Nijagunappa R and Venkataraman A, Synthesis and characterization of zinc ferrite nanoparticles obtained by self-propagating low-temperature combustion method, Bull. Mater. Sci., 2011, 34(7), 1325–1330.

13. Mahmoud Goodarz Naseri and Elias B. Saion, Crystalization in Spinel Ferrite Nanoparticles, *Advances in Crystallization Processes*, 2012, 349-380.
14. Ahmed M. El-Sayed and Esmat M. A. Hamzawy, Structure and Magnetic Properties of Nickel–Zinc Ferrite Nanoparticles Prepared by Glass Crystallization Method, *Monatshefte für Chemie*, 2006,137, 1119–1125.

\*\*\*\*\*